Visual colour inspection with a hyperspectral camera: inline application for automotive parts production

Eduardo Assunção[1], Magno Guedes[1] and Fábio Miranda[1]
1 Introsys SA, Portugal, e-mail: eduardo.assuncao@introsys.eu

Abstract

The development of cars is becoming increasingly focused on colour, which is a major challenge for both suppliers and manufacturers. Manufacturers must establish strict colour tolerances for each coloured component and specify both colour and appearance. On the other hand, suppliers must maintain colour accuracy in part production, regardless of the type of material used, to ensure acceptance of colour by automotive manufacturers. In the colour industry, colour difference formulas are used to make unbiased judgments about whether manufactured goods should be approved or disapproved. These objective judgments are based on instrumental colour measurements that must accurately predict subjective colour variations.
Hyperspectral imaging (HSI) has proven to provide helpful data for a variety of applications in numerous industries, including colour science.
To measure and analyse colour differences between automotive parts, we proposed to use conventional colour science algorithms in conjunction with the Specim FX10 hyperspectral camera, which has a flexible infrastructure that can receive data from a Generic Interface for Cameras (GenICam) compatible with the Gigabyte Ethernet interface.
The results showed that the use of hyperspectral imaging in production offers great potential for providing real-time colour information so that colour shifts can be detected early and costly errors in the production line can be avoided.

Keywords: Hyperspectral imaging, colour analysis, automotive industry

1. Introduction

Colour is becoming more significant in automotive design, which is a challenging issue for suppliers as well as manufacturers. Manufacturers must establish rigorous colour tolerances for each coloured component and specify both colour and look in order to create unambiguous expectations. Suppliers must maintain colour accuracy in aesthetic part production regardless of the type of material used to assure colour homogeneity and acceptability by automakers. Parts suppliers need reliable solutions to measure colour and verify colour harmony between different components before they are delivered to the manufacturer of vehicles [1] .

 https://doi.org/10.58286/28125

Currently, in the automotive industry, the colour quality control of an aesthetic or visible part is determined by characterizing the measured colour. For this purpose, commercially available devices such as the MA-5 QC [2], BYK-mac [3], and Nix Spectro 2 [4] are used. These devices measure samples in various geometries by contact. *Direct measurement* is the term for this method [5]. Since this is a manual method, it is impractical for use in a production line (see Figure 1). To solve this problem, an "indirect measurement" is required.

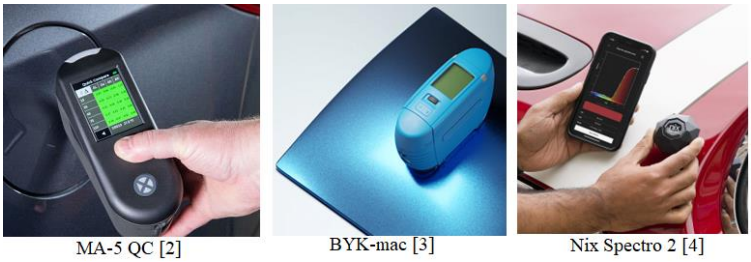

MA-5 QC [2] BYK-mac [3] Nix Spectro 2 [4]

Figure 1. Commercial colour measurement device

Gómez et al. [5] proposed an indirect colour measurement for the analysis of automotive paints using a telespectroradiometer PR-650 and a spectral cabinet with directional illumination (from BYK-Gardner). However, the method is not yet suitable for use in the production line. The reason for this is that the method was developed for conducting experiments in the laboratory.

In the colour domain, each spectral colour is defined by the wavelength of its light, and a common unit of measurement is the nanometer (nm). The primary colours are in the following wavelength ranges: Violet (450 nm and below), Blue (450-480 nm), Blue-Green (480-510 nm), Green (510-550 nm), Yellow-Green (550-570 nm), Yellow (570-590 nm), Orange (590-630 nm), and Red (630 nm and above) [6]. Based on this definition, a colour on a surface of a material can be characterized by measuring the spectral distribution of light (i.e., the reflectance curve). This can be done with the aid of a hyperspectral camera. Hyperspectral imaging (HSI) techniques have shown significant potential for a wide range of applications in diverse fields, from environmental research to precision agriculture. To create datasets with three dimensions, the spectral power distribution (SPD) is measured (or recovered) for each pixel of the image (also called data cube) [7]. Foster et al. [8] published a paper introducing terrestrial hyperspectral imaging and some of its applications in human colour vision research. They also describe image transformations for colorimetric displays and colour rendering. Magnusson et al [9] provided an algorithm that uses standardised techniques to generate realistic colour images from HSI. The algorithm converts each observable spectral band to a XYZ colour system, which is then converted to the standard red, green, and blue (sRGB) colour space. Two HSI datasets were used to validate the methodology. Morales et al. [10] described the commercially available Specim FX Hyperspectral Series scanning system (camera) (FX10 and FX17), which captures HSI samples for examination and processing to obtain the essential data on the spectral properties of the samples under study. Raza et al. [7] compared and evaluated three hyperspectral cameras in terms of their colorimetric accuracy. The study describes a formal setup for the characterisation of hyperspectral imaging devices. They use a 24-patch ColorChecker to evaluate the accuracy of HSI systems representing 24 natural colours.

In this paper, we propose to use the Specim FX10 hyperspectral scanning camera to measure and analyse colour differences between automotive parts. The contribution of

this article is to present a non-contact colour measurement that can be used in the inspection production line.

2. Materials and Methods

2.1 Hyperspectral imaging system

The HSI system used in this article was the FX10 line scan camera. In a single shot, the sensor can capture all spectral information in one dimension and spatial information in the other. An additional movable mechanism provides mechanical scanning of the entire given field of view and the ability to fill the third dimension of the data cube, allowing reconstruction of the original scene [7]. For more information about the FX10, see the user manual [11].
GPS antenna covers from motor vehicles were used for the experiments. Figure 2 illustrates the experimental setup. In (a), the camera, illumination, and scan line are represented by a drawn figure. In (b), the real setup developed for the experiment can be seen. The blue conveyor belt is used to transport the test samples.

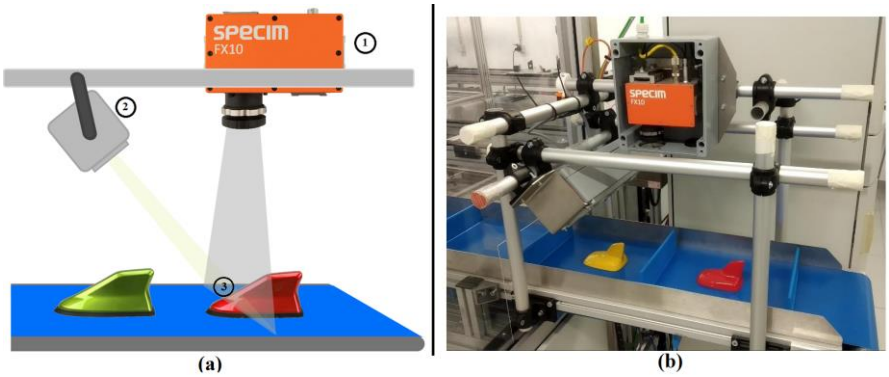

Figure 2. Experiment setup- (a): (1) FX10 hyperspectral camera, (2) Halogen Illumination, (3) scan line illustration. (b): Real prosed setup.

2.2 Computational resource

A desktop computer with a processor Intel® Core™ i3-3220 CPU @ 3.30GHz, RAM memory of 16.0 GB, running Windows 10 Professional OS was used to perform the experiments. Also, the Python interpreter was used with the libraries Harvesters for accessing and controlling the camera and Colour-science for the colour algorithms.

2.3 Data processing

The camera and the samples (antennas) are in the centre of the conveyor belt. This means that the centre of the scanned line coincides with the centre of the sample to be tested. Therefore, after a line acquisition, the spectral reflectance data associated with the 10 central pixels were extracted for analysis.
The colour science approach was used to perform the colour analysis based on the acquired spectral reflectance. Spectral reflectance was converted to tristimulus values CIE-XYZ (i.e., the portions of red-green-blue primary light that achieve colour match) using the CIE 2° fundamental observer colour match functions (CMFs) [12]. In addition, the values from XYZ were used to derive the CIE L*a*b* colour values, where L* stands for lightness and ranges from 0 to 100, and a* and b* stand for the red-green and yellow-

blue chromatic components, respectively, and range from -128 to 127. L*a*b* is a uniform colour space, i.e., a space in which the perceived colour differences are proportional to uniformly distributed points[8]. In summary, L*a*b values are numerical representations of colours.

2.4 Colour difference

For the comparison of colours (assessment), the colour difference Delta E (ΔE) is used and given as a single value. For this purpose, two colour values ($L_1 * a_1 * b_1$ and $L_2 * a_2 * b_2$) are used as input for the calculation of the ΔE [8]. The CIE76 colour difference formula is defined as:

$$\Delta E = \sqrt{(L_2 - L_1)^2 + (a_2 - a_1)^2 + (b_2 - b_1)^2}$$

According to the literature [13], a standard observer sees the colour difference as shown in Table 1.

Table 1. How a standard observer sees the difference in colour

ΔE	Perceptive difference in colour
0 <ΔE< 1	Observer does not notice the difference
1<ΔE<2	Only experienced observer can notice the difference
2<ΔE<3.5	Unexperienced observer also notices the difference
3.5<ΔE<5	Clear difference in colour is noticed
5<ΔE	Observer notices two different colours

3. Results and Discussion

Ten samples of car cover of antennas were used for the experiments (see Figure 3). The samples are in pairs (i.e., two samples have the same colour). This allows the evaluation of the proposed method in terms of accuracy. The reason is that samples that have the same perceptual colour also have very small ΔE-colour differences. Moreover, there are samples that differ slightly in perception. In this case, the ΔE must not be too small. Finally, colours that are very different in perception (e.g., yellow and red; red and blue) must have large ΔE.

Figure 3. Samples of car cover of antenna.

Table 2 shows the results of colour analysis between pairs of samples without perceptible colour differences. The pairs of L*a*b (measured) values are used to calculate the ΔE. The *white* samples yield the smallest ΔE (0.11), followed by the *grey* samples with a ΔE of 0.28. The *yellow* samples had the largest colour difference with a ΔE of 0.9. In this experiment, all ΔEs were less than one. According to the literature, humans cannot perceive a colour difference whose ΔE value is less than one (see Table 1). These results

are to be expected since the colour analyses were performed on samples of the same colour (e.g., white versus white, grey versus grey, etc.).

Table 2. Colour difference result (in pair of samples with no perceptual colours difference)

Sample	L*a*b	ΔE
White 1	86,72 * -1,51 * 3,3	0.11
White 2	86,66 * -1,46 * 3,2	
Gray 1	94,68 * -1,45 * 5,23	0.28
Gray 2	94,83 * -1,62 * 5,42	
Blue 1	18,25 * 12,52 * -36,41	0.39
Blue 2	18,6 * 12,05 * -35,49	
Red 1	46,1 * 57,11 * 35,83	0.47
Red 2	46,09 * 57,48 * 35,07	
Yellow 1	78,88 * 8,69 * 67,57	0.9
Yellow 2	79,51 * 8,41 * 64,45	

Table 3 shows the results of colour analysis between pairs of samples with perceived colour differences. Reference is made to Table 1 for some explanation. The colour difference (ΔE) for the white versus grey samples is 5.22. The colours are very close in perception. Therefore, a small ΔE value is expected, but it should be greater than 5 (since a significant colour difference is observed). Similar ΔE values (close to 45) are obtained for the yellow versus red and red versus blue samples. Large ΔE values are expected for these samples since the colours are very different. The blue and white samples are opposite colours. Therefore, the ΔE is the largest (71.91).

Table 3. Colour difference result (in pair of samples with perceptual colour difference)

Sample	L*a*b	ΔE
White	86.72 * -1.51 * 3.3	5.22
Gray	94.68 * -1.45 * 5.23	
Yellow	78,88 * 8,69 * 67,57	45.09
Red	46.1 * 57.11 * 35.83	
Red	46.1 * 57.11 * 35.83	44.28
Blue	18,25 * 12,52 * -36,41	
Blue	18,25 * 12,52 * -36,41	71.91
White	86,72 * -1,51 * 3,3	

4. Conclusions

In this study, a non-contact method designed to automate the qualitative colour analysis of automotive parts using a hyperspectral camera was proposed and described. The colour differences between samples were analysed, and the results are quite promising for the application of the proposed method to the inspection of automotive parts on the assembly line. The colour difference results confirm that the method can distinguish both slightly and strongly different colours.

An important practical aspect is that to analyse the sample as a whole, the camera must be moved according to the shape of the sample, since car parts are generally not flat. For this purpose, we propose to attach the camera to a robotic arm.

Acknowledgements

The research leading to these results has received funding from the Portuguese Government's Portugal 2020 PO CI innovation and development programme under grant agreement No 45077, project CheckMate (Development of a mobile checking station for characteristic analysis and structural testing after final assembly of automotive vehicles).

References and footnotes

[1] X-rite, "Color Measurement for Automotive Part Suppliers," 2022. https://www.xrite.com/industry-solutions/automotive/automotive-part-suppliers (accessed Aug. 18, 2022).

[2] X-rite, "MA-5 QC: Actionable Color Measurement Tool for Effect Finishes," 2022. https://www.xrite.com/categories/portable-spectrophotometers/ma-family/ma-5_qc (accessed Oct. 27, 2022).

[3] BYK, "Multi-angle color measurement," 2022. https://www.byk-instruments.com/en/Multi-angle-color-measurement/c/p-32719 (accessed Oct. 27, 2022).

[4] Nix, "Nix Spectro 2 Spectrophotometer." https://www.nixsensor.com/nix-spectro/ (accessed Nov. 15, 2022).

[5] O. Gómez *et al.*, "Visual and instrumental assessments of color differences in automotive coatings," *Color Res. Appl.*, vol. 41, no. 4, pp. 384–391, Aug. 2016, doi: 10.1002/col.21964.

[6] "Spectral Colour Reproduction," in *The Reproduction of Colour*, Chichester, UK: John Wiley & Sons, Ltd, 2005, pp. 1–8. doi: 10.1002/0470024275.ch1.

[7] A. Raza, D. Dumortier, S. Jost-Boissard, C. Cauwerts, and M. Dubail, "Accuracy of Hyperspectral Imaging Systems for Color and Lighting Research," *LEUKOS*, pp. 1–19, Jun. 2022, doi: 10.1080/15502724.2022.2067866.

[8] D. H. Foster and K. Amano, "Hyperspectral imaging in color vision research: tutorial," *J. Opt. Soc. Am. A*, vol. 36, no. 4, p. 606, Apr. 2019, doi: 10.1364/JOSAA.36.000606.

[9] M. Magnusson, J. Sigurdsson, S. E. Armansson, M. O. Ulfarsson, H. Deborah, and J. R. Sveinsson, "Creating RGB Images from Hyperspectral Images Using a Color Matching Function," in *IGARSS 2020 - 2020 IEEE International Geoscience and Remote Sensing Symposium*, Sep. 2020, pp. 2045–2048. doi: 10.1109/IGARSS39084.2020.9323397.

[10] A. Morales *et al.*, "Laboratory Hyperspectral Image Acquisition System Setup and Validation," *Sensors*, vol. 22, no. 6, p. 2159, Mar. 2022, doi: 10.3390/s22062159.

[11] Specim, "Specim FX10 - User Manual," 2022. https://www.stemmer-imaging.com/media/uploads/cameras/specim-spectral-imaging/16/161584-Specim-FX10-Reference-Manual.pdf (accessed Nov. 15, 2022).

[12] "Colorimetry," in *Color Appearance Models*, Chichester, UK: John Wiley & Sons, Ltd, 2013, pp. 56–84. doi: 10.1002/9781118653128.ch3.

[13] W. S. Mokrzycki and M. Tatol, "Colour differenceΔ E-A survey," *Mach. Graph. Vis*, vol. 20, no. 4, pp. 383–411, 2011.